Estimating Vehicle Interior Noise Using Room Models and Sound Power

Lee E. Schroeder, International Truck and Engine Corporation, Fort Wayne, Indiana

In this article, interior noise of a large commercial truck was modeled with the room equation. This approach assumed that integrated-sleeper truck cabins may be adequately modeled as a practical room. The method is used in architectural acoustics studies, where ray theory and statistical concepts are suitable and where application of complicated wave theory may not be necessary. This simplifies computational requirements, making a semi empirical scheme useful for timely product development. The study employed sound power measurements at thirty-four surface patches encompassing the interior cabin boundary. Each surface patch constituted an individual interior noise source. Predicted and measured results correlated well, demonstrating the capability to estimate driver-position noise level from predicted periphery sound intensity changes.

Commercial trucks equipped with integral-sleepers offer large interior volume as compared to passenger car applications. An example is the International® Hi-Rise Pro Sleeper® cab, illustrated in Figure 1. Cavity volume of approximately 15 m^3 is typical. Low-frequency sound intensity measurements may be made with improved accuracy as the sound field is less reverberant. This case study presents useful incoming sound power measurements and noise prediction through the 160 to 5000 Hz 1/3-octave bands. Sound power measurements at thirty-four discrete surface patches encompassed the interior driver space. Each periphery surface patch constituted an individual interior noise source. Unlike previous studies, the room equation was empirically determined to obtain a typical best fit formulation. This allowed the prediction of driver position sound pressure level from periphery incoming sound power. Equivalent room-equation parameters were calculated by a least squares scheme using multiple measurement sets. By treating the baseline condition with subsequent passive noise control materials and by isolating flanking paths, the interior noise was sequentially reduced by approximately 5 dB; each data set was within this range.

Experimental Procedure

All measurements were completed in an International 9400 Pro Sleeper. This is a contemporary example of a Class-8 integral sleeper tractor. Reported sound pressure levels were made according to CFR Title 49, Part 393.94. The test method represents stationary conditions at governed high idle, approximately 6 in. to the right of the driver's ear. Corresponding acoustic intensity data included spatial and time averaged measurements over thirty-four boundary patches and essentially created an enclosed envelope around the driver space. The rear boundary represented an imaginary plane separating the front driver space and sleeper berth. All intensity measurements were near field, normally orientated and approximately 100 mm from each surface. Figure 2 offers an illustration of the geometry. The boundary panels are opened in this view to better illustrate interior detail.

Since the top and rear of the cab were open paths to the sleeper compartment, these two areas, denoted by surface-32 and surface-33, were imaginary boundary planes. Note that boundary areas under the seat bases were inaccessible and absorption existed within the envelope *via* the seats and occupant. Measurement instrumentation included a Brüel & Kjær Type 2144 portable two-channel analyzer. Sound intensity measurements utilized two spacers to encompass the frequency range of interest and phase error was corrected by prior residual intensity compensation. Sound level at the driver position was successively reduced to a total reduction of approximately 5 dB. This was achieved by incorporating improved barrier treatment, adding panel damping, removing structural paths, etc. Fifteen sets of complete sound intensity/sound pressure measurements were recorded.

Measurement Error and Limitations. Practical sound intensity measurement is influenced by many sources of error. Prior planning becomes necessary in order to ensure measurement integrity. Two sources of error, specifically bias and random, can be estimated directly; others are more difficult to access. Miscellaneous error sources were introduced by practical measurement limitations such as: measurement probe accessibility and poor signal-to-noise ratio for several patch sources. See Reference 2 for additional information on error sources. In addition, it was recognized that low frequency source repeatability was lacking during some test conditions.

Bias error derives from two primary sources: finite difference approximation and phase mismatch effects. Finite difference approximation degrades (underestimates) sound intensity measurements toward the higher frequency limit. Phase mismatch particularly degrades low frequency accuracy. Phase mismatch is important to consider for near-field measurements, highly reactive or diffuse fields, small microphone spacing and cases where the sound field is incident at an angle to the probe axis. Measurements in these types of situations demand a well phase-matched and magnitude-matched microphone pair. Figure 3 illustrates typical error bounds calculated from formulations and tables available in Reference 3. The random error component was based on 68% confidence levels for 40 sec averaging times. Note that all analysis and modeling efforts presented by this work only considered measurements through the 160-5000 Hz 1/3 octave bands. Here, sound intensity error was less than ±1 dB through the 250-5000 Hz bands; and approximately ±2 dB through the 160-200 Hz bands. This error estimate assumed uncorrected phase mismatch, but actual measurements were automatically adjusted by residual intensity compensation.

Sound Field Characteristics. The sound field in a truck cabin was examined by considering the relationship between driver-position sound pressure and the acoustic energy entering the cabin space through the periphery boundary. The sound field at any instant is complex, composed of direct (free-field) and indirect (reflected or diffuse) wave fronts. Standing waves may also be present under certain conditions. Figure 4 illustrates measured acoustic energy density at the driver's ear for a typical configuration. Generally, the diffuse-field dominates but direct-field contribution becomes more important at higher frequencies where boundary absorption is significant.

Predicting SPL from Boundary Acoustic Intensity

The simple mathematical model presented here provides a means to predict local driver-position sound level, given spatially averaged incoming sound energy emanating through a finite number of boundary patches; Figure 2 offers an illustration. Once measurements are available, as in this example, analytical formulations may be used to predict effects of proposed (arbitrary) interior package changes. In addition, sepa-

Based on paper number 2001-01-1533 © 2001 Society of Automotive Engineers, Inc. Presented at the 2001 SAE Noise & Vibration Conference & Exposition, Traverse City, MI, April/May 2001.

Figure 1. International® 9400i Class-8 tractor with the High-Rise Pro Sleeper®. Integrated-sleeper height of 196 cm by 183 cm deep.

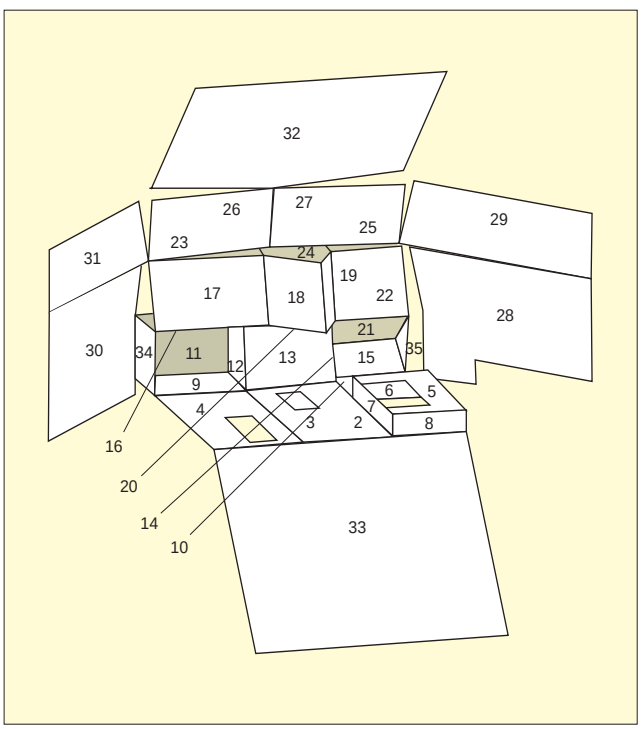

Figure 2. Driver environment boundary. Ceiling boundary, rear boundary, and doors are folded back to view the driver space.

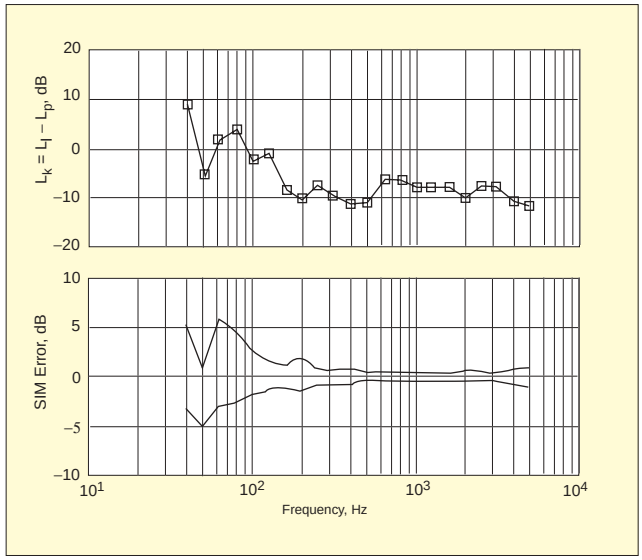

Figure 3. Reactivity index and maximum estimated SIM error bounds for Surface-2 in the original test condition. Calculated error is composed of phase mismatch, finite difference approximation and random sources.

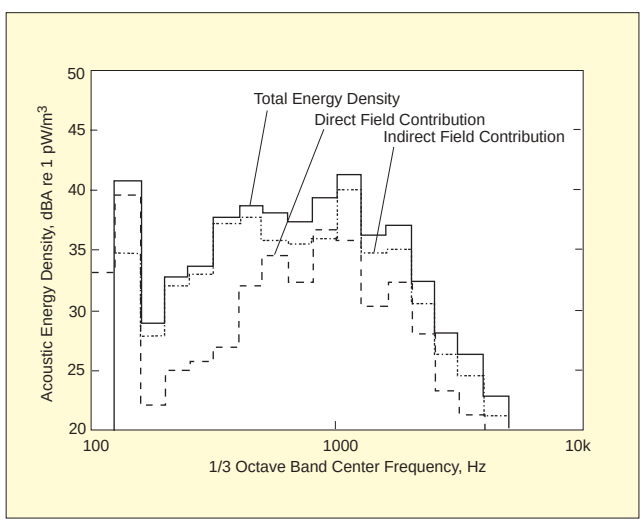

Figure 4. Acoustic energy density at the driver position for stationary high idle.

rate models are provided for the low- and high-frequency ranges. This allows a convenient means to predict separate modifications influenced by structural and airborne paths. Structural paths dominated interior noise contribution through the lower 1/3-octave bands to 500 Hz, while airborne paths governed the high-frequency range (630-5000 Hz bands). The overall noise change is the sum of the predicted low- and high-frequency results.

Sound intensity is a vector quantity and the probe axis for all measurement areas was normal to the panel surface or boundary plane. Thus, magnitude and energy-flow direction was known, so that incoming energy may be calculated by using the associated patch surface areas.

The interior sound field was modeled by superimposing free-field and diffuse-field representations as is done with a sound source in a practical room. Reference 1 describes a similar application. Noise sources were considered to be the incoming energy originating from boundary patches as illustrated in Figure 2. For the test method, the following model assumed the acoustic field to be stationary with respect to time and neglected the influence of standing waves. No significant sources were assumed to be located within this envelope. Absorption within the cavity was ignored, including dissipation by the seats, occupants and by the air space. Also, the prediction point (driver's ear) was assumed to be in the far-field of each source; hence, the low frequency situation was idealized. Finally, boundary area patches were treated as incoherent acoustic sources within the frequency range of interest. It was determined that coherence effects prevented the usefulness of this modeling scheme for energy contribution which is below the 160 Hz 1/3-octave band.

The diffuse field contribution was calculated to be proportional to the sum of the incoming acoustic energy. The free-field contribution also considers spherical wave front dispersion, according to the inverse-square law. The simplified model is represented as:

$$\frac{\hat{p}_{rms}^2}{\rho_0 c_0} = \sum_{i=1}^{n} (I_{IN})_i s_i \left[\frac{Q}{4\pi r_i^2} + \frac{4}{R} \right]$$

Here, Q is a nondimensional 'quasi' directivity factor and R is a 'quasi' room constant. These parameters are referred to as 'quasi' since they are not calculated or measured directly. Predicted sound pressure and measured sound intensity values are A-weighted representations given by:

$$\hat{L}_{pA} = 10\log_{10}\left(\frac{\hat{p}_{rms}^2}{p_{ref}^2}\right) \text{ and } (\mathrm{L_{IA}})_i = 10\log_{10}\left(\frac{(I_{IN})_i}{I_{ref}}\right)$$

Predicted sound level is the contributed energy-sum of each

Table 1. Room equation parameters from least-squares regressions.

Results from (15) Data Sets		Free- & Diffuse-Field Model	Free-Field Model	Diffuse-Field Model
Low Frequency 160-500 Hz Bands	Q	–1.6	7.1	N/A
	$R(m^2)$	7.6	N/A	9.3
High Frequency 630-5k Hz Bands	Q	–1.7	5.8	N/A
	$R(m^2)$	8.3	N/A	11
Overall 160-5k Hz Bands	Q	–2.3	6.2	N/A
	$R(m^2)$	7.3	N/A	10

Table 2. 95% confidence limits for best-fit room constant R.

95% Confidence Limits from Regression	Diffuse-Field Model, $R(m^2)$
Low Frequency 160-500 Hz Bands	6.3 - 17
High Frequency 630-5k Hz Bands	7.7 - 17
Overall 160-5k Hz Bands	7.7 - 14

i^{th} surface area s_i at a distance r_i from the prediction point. The term $r_o c_o$ denotes air characteristic impedance. The room parameters R and Q were determined by least-squares regression of fifteen sound intensity surveys at high-idle. Predicted overall levels comprised the sum of low and high frequency calculations. Error was minimized on an energy-basis.

Three models were examined. The first variation utilized least squares regression for the directivity factor and room constant. Two additional models assume diffuse or free field representations, only. Calculated regression parameters are listed in Table 1.

The general model, considering both diffuse and free field contributions yielded regression parameters with large statistical variation. This was due to the fact that both terms were highly correlated. Best correlation was found with the diffuse representation; statistical validation is summarized as follows.

Model Validation and Statistical Considerations

Low frequency and high frequency models may be chosen independently based on sound field characteristics. In this study, the diffuse model yielded the best model correlation. This was supported by the fact that the acoustic field was predominantly diffuse, as represented in Figure 4. In fact, it was also determined that the free-field representation exhibited improved correlation through the high-frequency range, rather than through the low, supporting the acoustic energy distribution measured at the driver position.

Validation of model formulation was considered with various statistical measures. The regression null hypothesis test demonstrated basic diffuse field model relationship. There existed less than 0.5% risk of error to conclude that the basic relationship exists based on the statistical significance between measured sound power and interior noise at the driver's ear. The multiple correlation coefficient defines the fraction of the total variation of the predicted sound level attributed to its regression on the incoming acoustic energy. Results demonstrated that measured incoming sound power and cavity sound pressure were well correlated as values were close to the perfect correlation value of one, ranging from 0.8 to 0.9.

Additional measures were utilized to quantify model performance. Standard error of the estimate quantifies scatter of measured values about the regression equation. Standard error was approximately 62 dB for the each 1/3-octave band frequency range, bounded by approximately ±1.5 dB from the overall regression curve.

Table 2 summarizes 95% confidence limits for the room constant of the diffuse energy representation. This describes uncertainty associated with parameter determination in this experimental sample.

As an example case, Table 3 lists predicted noise level values with corresponding confidence limits. Predicted estimates presume known total incoming sound power of 77 dB(A). This model would prove useful for assessing interior noise level effects incurred by estimated noise control component changes.

Table 3. 95% confidence limits for predicted noise level: example case.

	Known Incoming Sound Power	Predicted Noise Level from Diffuse Model	Predicted 95% Confidence Limits, dBA
Low Frequency 160-500 Hz Bands	74 dBA	70.5 dBA	68.6 - 71.8
High Frequency 630-5k Hz Bands	74	69.9	68.1 - 71.2
Overall 160-5k Hz Bands	77	73.2	72.0 - 74.1

Conclusion

The practical room equation was successfully applied for heavy truck interior noise prediction. Specifically, where the diffuse energy field dominates, the indirect term is sufficient for interior noise level estimates. This scheme may be particularly useful when estimating noise level changes incurred by known or estimated sound power modifications at the component level.

References

1. Atwal, M., Heitman, K., and Crocker, M., "Prediction of Light Aircraft Interior Sound Pressure Level from the Measured Sound Power Flowing Into the Cabin," Inter-Noise Proceedings, 1986.
2. Gade, S., "Sound Intensity (Part I. Theory)," *Brüel & Kjær Technical Review*, No. 3 - 1982.
3. Gade, S., "Validity of Intensity Measurements in Partially Diffuse Sound Field," *Brüel & Kjær Technical Review*, No. 4 - 1985.
4. Crow, E., Davis, F., and Maxfield, M., *Statistics Manual*, Dover Publications, 1960.

The author can be contacted at: lee.schroeder@nav-international.com.